Available online at www.sciencedirect.com

ScienceDirect

Procedia Manufacturing 47 (2020) 696–701

Procedia MANUFACTURING

www.elsevier.com/locate/procedia

23rd International Conference on Material Forming (ESAFORM 2020)

From Component Reduced Models to Reduced Modelling of Multi-Component Systems

Giacomo Quaranta[a]*, Mustapha Ziane[b], Simó Masqué Barri[a], Carlos Terres Aboitiz[a], Anne Chambard[b], Jean Louis Duval[b], Elias Cueto[c], Francisco Chinesta[d]

[a]*ESI Group Hispania, Calle de Francisca Delgado, 11, 28108 Alcobendas, Madrid, Spain.*
[b]*ESI Group, 3bis rue Saarinen, 94528 Rungis CEDEX, France.*
[c]*Universidad de Zaragoza, Edificio Betancourt. Maria de Luna, s.n., 50018, Zaragoza, Spain.*
[d]*ENSAM ParisTech, 151 rue de l'Hôpital. 75013 Paris, France*

* Corresponding author. *E-mail address:* Giacomo.Quaranta@esi-group.com

Abstract

The present work focuses on the reduced modelling of multi-component systems, in particular on a two stages stamping chain process. Starting from snapshots collected by using the commercial software PAM-STAMP, the non-intrusive sparse-PGD constructor is used in order to build a parametric transfer function of each operation in a separated representation, circumventing the problem of the curse of dimensionality. Moreover, in order to fill the gap between this deterministic solution and the measured fields and safely applied control strategies, data driven-modeling can be employed according to the new "hybrid twin" methodology.

Keywords: stamping; hybrid-twin; model order reduction; PGD.

1. Introduction

Since the previous (third) industrial revolution numerical simulation has been widely used in many scientific and engineering fields, defining the so called "virtual twins". They make possible the virtual evaluation of systems responses, from the accurate solution of the mathematical model expected describing it (by using methods as finite differences, finite elements, finite volumes, …) [1]. However, usually virtual models are static, that is, they are used in the design of complex systems and their components, but they are not expected to accommodate or assimilate data. The characteristic time of standard simulation strategies is not compatible with the real-time constraints compulsory for control purposes; moreover optimization and inverse analyses involved in calibration procedures require respectively many direct calculations to find the optimal or the searched parameters.

Thus Model Order Reduction techniques (POD, PGD, reduced basis, …) [2, 3, 4, 5, 6, 7, 8] opened new possibilities for more efficient simulations allowing important computing-time savings, of several orders of magnitude in some cases, making possible the construction of very general solutions (parametric in many cases) able to ensure almost instantaneous responses to queries and the assimilation of data collected from sensors into the physically-models, defining the so called "digital twins".

2. Parametric model

The two-stages stamping process depicted in Fig. 1 is analyzed and its control described. The first stage proceeds from a plate shell, whereas the second one acts on the part that results from the first stage, fact that implies the necessity of properly address the link between both stages.

10.1016/j.promfg.2020.04.214

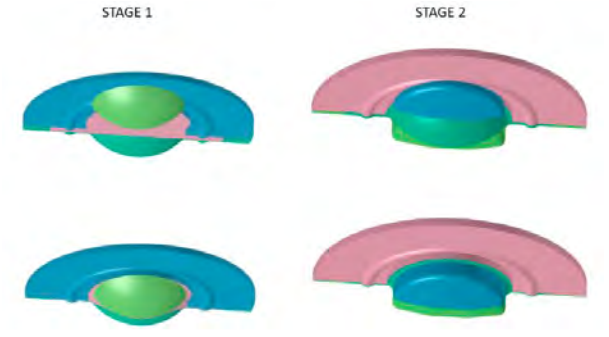

Fig. 1. Two-Stage Stamping: (left) first stage; (right) second stage; (top) initial configuration and (bottom) final one.

Three process parameters are considered in each stage: (i) the closing force F, (ii) the friction coefficient ξ between the sheet and the tooling and (iii) the one μ between the sheet and the flan-clamping. Thus, for the first stage the parametric expression of the thermo-mechanical state reads

$$X^I(\boldsymbol{x}, F^I, \xi^I, \mu^I) \tag{1}$$

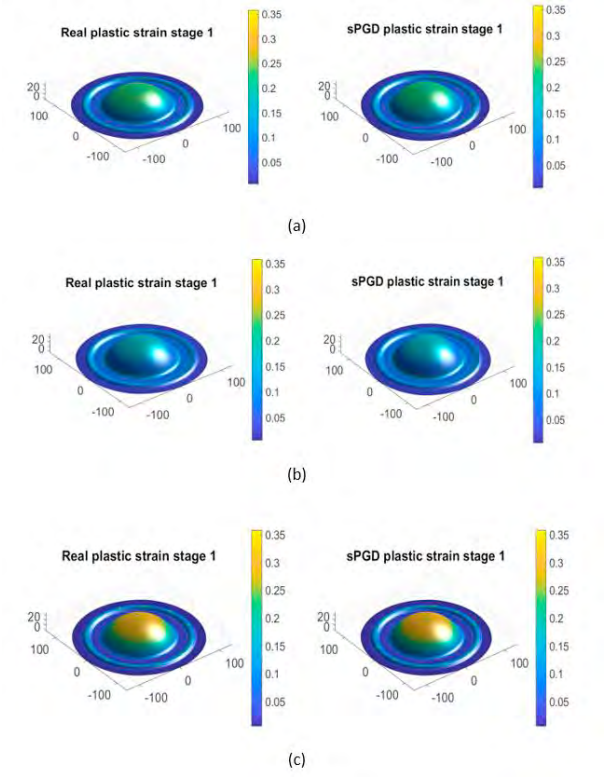

Fig. 2. Real (left) and predicted (right) displacement and plastic strain at the end of the first stage for three different combinations of the parameters F^I, ξ^I and μ^I.

where $\boldsymbol{x}$ is the spatial coordinate and the superscript $\blacksquare^I$ refers to the first stage of the global process. In this work this parametric solution is constructed by combining PAM-STAMP and the s-PGD constructor [9] (some details on the sPGD method are given in Appendix A) which allows to write the mechanical state in its separated representation

$$X^I(\boldsymbol{x}, F^I, \xi^I, \mu^I) = \sum_{i=1}^{N} \Lambda_i^I(\boldsymbol{x}) \Phi_i^I(F^I) \Psi_i^I(\xi^I) \mathrm{P}_i^I(\mu^I). \tag{2}$$

This can be seen as a transfer function for the first stage: given a set of parameters $(\hat{F}^I, \hat{\xi}^I, \hat{\mu}^I)$, the output is fully determined by (2). Figs. 2 and 3 depict three different particularizations of the parametric solution (2) at the end of the first stage for three different arbitrary choices of the parameters. The reduced model solution is a good approximation of the full model one. Let's note that, in the case we were also interested in the time evolution of the state along the stage, we could simply add the time as an extra parameter and looking for the corresponding modes in the separated representation (2).

The parametric solution of the second stage operates on the part coming from the first stage, so that its initial state should be also included as an extra parameter, i.e.

$$X^{II}(\boldsymbol{x}, F^{II}, \xi^{II}, \mu^{II}, X^I(\boldsymbol{x})). \tag{3}$$

Being $X^I(\boldsymbol{x})$ fully determined by the three process parameters of the first stage one possible solution would be to express the state, using again the s-PGD constructor, as

$$X^{II}(\boldsymbol{x}, F^I, \xi^I, \mu^I, F^{II}, \xi^{II}, \mu^{II}) = \sum_{i=1}^{N} \Lambda_i^{II}(\boldsymbol{x}) \Phi_i^{II}(F^I) \Psi_i^{II}(\xi^I) \mathrm{P}_i^{II}(\mu^I) \Theta_i^{II}(F^{II}) \Gamma_i^{II}(\xi^{II}) \mathrm{E}_i^{II}(\mu^{II}). \tag{4}$$

Given an input state $\hat{X}^I(\boldsymbol{x})$, either the corresponding first stage parameters $(\hat{F}^I, \hat{\xi}^I, \hat{\mu}^I)$, are known or, in the case they are not, they can be determined from (2) by imposing that

$$(\hat{F}^I, \hat{\xi}^I, \hat{\mu}^I) = \underset{(F^I, \xi^I, \mu^I)}{\operatorname{argmin}} \left\| \hat{X}^I(\boldsymbol{x}) - \sum_{i=1}^{N} \Lambda_i^I(\boldsymbol{x}) \Phi_i^I(F^I) \Psi_i^I(\xi^I) \mathrm{P}_i^I(\mu^I) \right\|_2. \tag{5}$$

Thus, by imposing $F^I = \hat{F}^I$, $\xi^I = \hat{\xi}^I$ and $\mu^I = \hat{\mu}^I$ in (4) we have that

$$X^{II}(\boldsymbol{x}, F^{II}, \xi^{II}, \mu^{II}, \hat{X}^I(\boldsymbol{x})) = \sum_{i=1}^{N} \gamma_i \Lambda_i^{II}(\boldsymbol{x}) \Theta_i^{II}(F^{II}) \Gamma_i^{II}(\xi^{II}) \mathrm{E}_i^{II}(\mu^{II}) \tag{6}$$

where

$$\gamma_i = \Phi_i^{II}(\hat{F}^I) \Psi_i^{II}(\hat{\xi}^I) \mathrm{P}_i^{II}(\hat{\mu}^I). \tag{7}$$

This can be seen as a transfer function for the second stage process. In fact, given an input state $\hat{X}^I(\boldsymbol{x})$ and a set of parameters $(\hat{F}^{II}, \hat{\xi}^{II}, \hat{\mu}^{II})$ the output is fully determined by (6). Figs. 4 and 5 depict three different particularizations of the parametric solution (2) at the end of the second stage for three different arbitrary choices of the parameters describing the thermo-mechanical state of the incoming part (the three combinations of Figs. 2 and 3) and the second stage parameters. Again, the reduced model solution is a good approximation of the full model one.

However, when the number of process stages increases, at each new stage more parameters have to be taken into account (the ones of all the previous stages). The fact of using too many parameters require a higher computational effort for building

the parametric solution of the corresponding stage and at the same time reduce the precision and the efficiency of the reduced solution built with the sPGD technique.

In order to avoid this, a good alternative to the previous method consists in parametrized the incoming thermo-mechanical state of a particular stage using the coefficients of the most relevant modes coming from a linear or nonlinear dimensionality reduction analysis performed on a training based on the previous stage parametric solution.

In the example of Fig. 1, taken into consideration in this work, a Proper Orthogonal Decomposition (POD) technique [5] was performed on the same states (i.e. at the end of the first stage) used to build the parametric solution (2). Only two modes were revealed to be important, so that, given an input state $X^I(\boldsymbol{x})$, it can be parametrized as

$$X^I(\boldsymbol{x}) \;=\; \alpha \mathrm{X}_1(\boldsymbol{x}) + \beta \mathrm{X}_2(\boldsymbol{x}), \tag{8}$$

where $\mathrm{X}_1(\boldsymbol{x})$ and $\mathrm{X}_2(\boldsymbol{x})$ are the two modes computed with the POD. The state at the end of the second stage can then be expressed using the sPGD constructor as

$$X^{II}(\boldsymbol{x},\alpha,\beta,F^{II},\xi^{II},\mu^{II}) = \sum_{i=1}^{N} \Lambda_i^{II}(\boldsymbol{x}) A_i(\alpha) B_i(\beta)\, \Theta_i^{II}(F^{II}) \Gamma_i^{II}(\xi^{II}) \mathrm{E}_i^{II}(\mu^{II}). \tag{9}$$

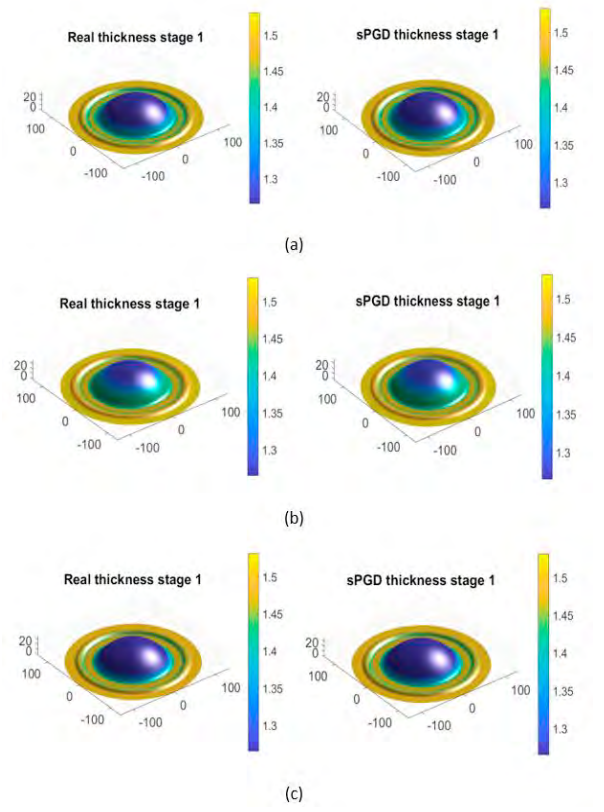

Fig. 3. Real (left) and predicted (right) displacement and thickness at the end of the first stage for three different combinations of the parameters F^I, ξ^I and μ^I (same as Fig. 2).

Thus, given an input state $\hat{X}^I(\boldsymbol{x})$, the parameters $(\hat{\alpha},\hat{\beta})$, corresponding to its parametrization, are computed by projecting it on the reduced base composed of the two modes $\mathrm{X}_1(\boldsymbol{x})$ and $\mathrm{X}_2(\boldsymbol{x})$. By imposing $\alpha = \hat{\alpha}$ and $\beta = \hat{\beta}$ in (9) we have again (6) but where

$$\gamma_i = A_i(\hat{\alpha}) B_i(\hat{\beta}). \tag{10}$$

As already mentioned, (6) is a transfer function for the second stage process. The advantage of this second method is that the number of parameters does not increase as the number of stages increases since only the most important modes are taken into consideration at the beginning of each stage. In the example presented in this work, for instance, the numbers of parameters at the second stage reduced from 6 to 5, but a huger reduction can be obtained if many stages are considered (as it will be analyzed in future ongoing works). Moreover, given a new input, a simple projection on the reduced basis has to be performed in order to get the corresponding coefficients. Figs. 6 and 7 depict three different particularizations of the parametric solution (2) at the end of the second stage for the same choices of the parameters of Figs. 4 and 5. The results obtained with the reduced model are again an excellent estimation of the high-fidelity solution.

3. Future work: towards real-time control

In what follows we consider one of the possible controls among the large number of possible choices. The nominal first process parameters are assumed determined offline, $(F^I_{nom},\xi^I_{nom},\mu^I_{nom})$, and the expected solution at the end of the first stage is $X^I(\boldsymbol{x},F^I_{nom},\xi^I_{nom},\mu^I_{nom})$. However, a certain lack of accuracy is expected concerning the friction coefficients values and then, the accuracy of the first stage predictions has to be checked. For that purpose, some measurements are performed on the part leaving the first stage, before it enters in the second one and the gap between prediction and measurement is used for updating the first stage parametric model.

For this purpose, parameters ξ^I and μ^I are updated by enforcing that the associated predictions agree as much as possible with the experimental measurement. Indeed, updated parameters denoted by $\bar{\xi}^I$ and $\bar{\mu}^I$ allow updating the first stage parametric model that now reads

$$\bar{X}^I(\boldsymbol{x}) = X^I(\boldsymbol{x},F^I_{nom},\bar{\xi}^I,\bar{\mu}^I). \tag{11}$$

However, in practice, some deviations between the predicted and observed responses are usually noticed due to inaccuracies in the employed models, that sometimes are not accurate enough descriptions of the real systems, or to an a priori almost unpredictable time evolution of certain models. A certain part of the deviation (its unbiased component in a statistical sense) can be viewed as a noise and addressed by using adequate filters [10], but the remaining biased part proves the existence of a hidden model that operates but escapes to our understanding. In order to address this problem and efficiently attained system control, one possibility consists in constructing “on-the-fly” a data-driven model able to fill the gap between model prediction and measurement. This is the new **Hybrid Twin** paradigm [12, 11], in fact, as soon as the data-driven model allows making accurate predictions, i.e. improving the accuracy of $\bar{X}^I(\boldsymbol{x})$ in

(11), control strategies can be safely applied. The data-based deviation model can be built on-the-fly, directly from the collected data, by using machine learning techniques and artificial intelligence (data mining, deep learning, manifold learning, tensor learning, dictionary learning, linear and nonlinear regression … for citing few) [13, 14, 15].

Now, the predictions of the second stage when using its nominal process parameters and the updated input sate is

$$X^{II}(\boldsymbol{x}, F^{II}_{nom}, \xi^{II}_{nom}, \mu^{II}_{nom}, \bar{X}^{I}(\boldsymbol{x})). \quad (12)$$

The thermo-mechanical state at the end of the second stage can be checked (maximum plastic deformation and its associated damage, minimum thickness, ...) and if a risk is detected, the control system proceeds to look for the optimal force $\bar{F}^{II}$ fulfilling design criteria and avoiding forming defects. This search can be performed in real-time because the solution for each possible value of F^{II} only requires a simple particularization.

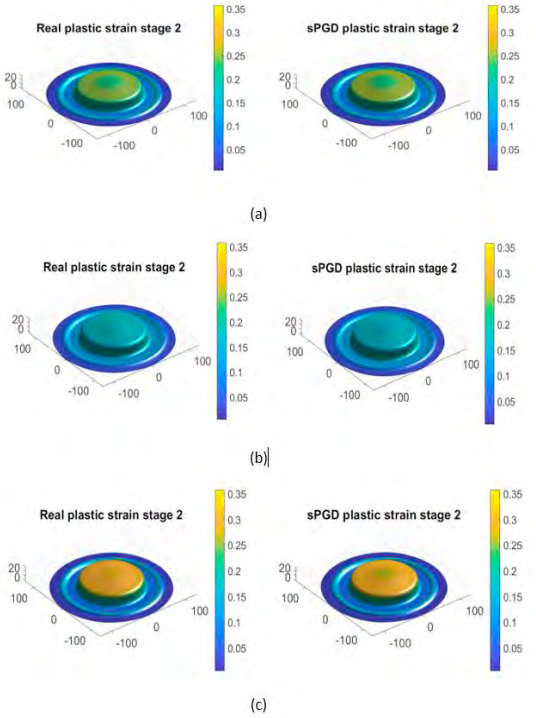

Fig. 4. Real (left) and predicted (right) displacement and plastic strain at the end of the second stage for three different combinations of the parameters F^{I}, ξ^{I}, μ^{I} (same as Figs. 2 and 3), F^{II}, ξ^{II} and μ^{II}.

The updated prediction that takes into account the real incoming part and also the updated force $\bar{F}^{II}$ writes

$$X^{II}(\boldsymbol{x}, \bar{F}^{II}, \xi^{II}_{nom}, \mu^{II}_{nom}, \bar{X}^{I}(\boldsymbol{x})). \quad (13)$$

However, here again, an uncertainty remains about the friction coefficients of the second stage process ξ^{II} and μ^{II}. In order to better calibrate both them, new measurements are performed on the part leaving the second stage, that allow calculating again in real-time the best value $\bar{\xi}^{II}$ and $\bar{\mu}^{II}$ of both parameters to make compatible prediction and measurement. As soon as both parameters have been identified, the second stage parametric model reads

$$\bar{X}^{II}(\boldsymbol{x}) = X^{II}(\boldsymbol{x}, \bar{F}^{II}, \bar{\xi}^{II}, \bar{\mu}^{II}, \bar{X}^{I}(\boldsymbol{x})). \quad (14)$$

Again, when parameters updating do not suffices, i.e. their updating is not enough for ensuring accurate enough predictions, the gap can be explained from a data-based deviation model that will be enriched each time that a new unexpected gap occurs and use to improve the accuracy of $\bar{\boldsymbol{X}}^{\boldsymbol{II}}(\boldsymbol{x})$.

The process model should be updated continuously, for each part coming into the two-stage stamping process, in order to ensure the quality of the produced parts.

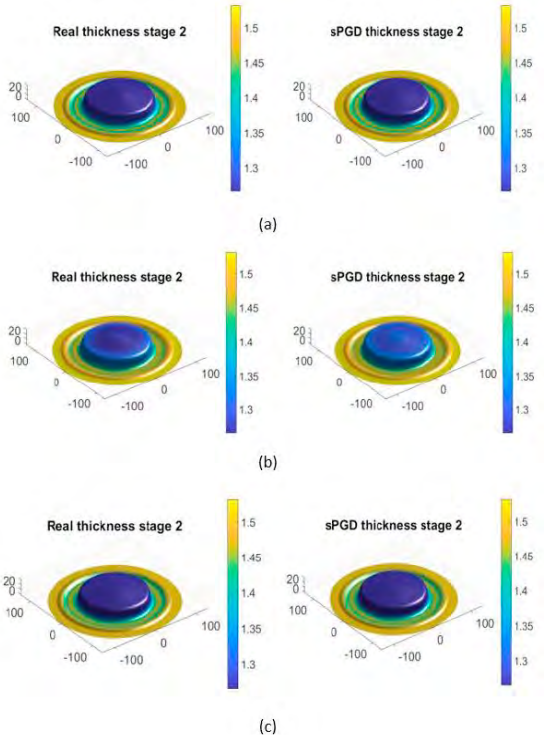

Fig. 5. Real (left) and predicted (right) displacement and plastic thickness at the end of the second stage for three different combinations of the parameters F^{I}, ξ^{I}, μ^{I} (same as Figs. 2 and 3), F^{II}, ξ^{II} and μ^{II} (same as Fig. 4).

4. Conclusions

This paper presented a reduced modelling of a multistep stamping chain process. The non-intrusive sPGD constructor was used in combination with the commercial software PAM-STAMP in order to build a parametric transfer function of each stage. Moreover, a dimensionality reduction technique was used for taking into account at a certain stage the thermo-mechanical state of the part coming from the previous stage. The numerical results showed how the predictions of the reduced model agree with the full order solutions. Finally, it is showed how the reduced modeling can be used for safe and efficient process control strategies by performing parameters

updating and by adding a data-driven correction in order to consider the physics that occurs during the process but that have not been taken into account in the simulations, according to the Hybrid Twin paradigm.

In this paper we took into consideration a two-stages stamping process, but the proposed methodology can be applied to more complex processes with much more stages and parameters. The application of the methodology to a multi-step hot stamping process constitutes a work in progress.

Appendix A. Sparse PGD: sPGD

The sPGD is a procedure for sparse approximation in high dimensional settings [9]. For the case of the exposition let assume that the unknown objective function $f(x,\mu,\eta)$ lives in $\mathbb{R}^3$, where x is the spatial coordinate and (μ,η) are the parametric coordinates, and that is to be recovered from sparse data. For that purpose we consider the Galerkin projection in $\Omega = \Omega_x \times \Omega_\mu \times \Omega_\eta$

$$\int_\Omega w(x,\mu,\eta)\big(u(x,\mu,\eta) - f(x,\mu,\eta)\big)dxd\mu d\eta = 0 \qquad (15)$$

where $\Omega \subset \mathbb{R}^3$ and $w(x,\mu,\eta) \in \mathcal{C}^0(\Omega)$ is an arbitrary test function. Following the Proper Generalized Decomposition (PGD) rationale [5], the next step is to express the approximated function $u^M(x,\mu,\eta) \approx u(x,\mu,\eta)$ in a separated form and looking for the enriched approximation $u^M(x,\mu,\eta)$ assuming known $u^{M-1}(x,\mu,\eta)$,

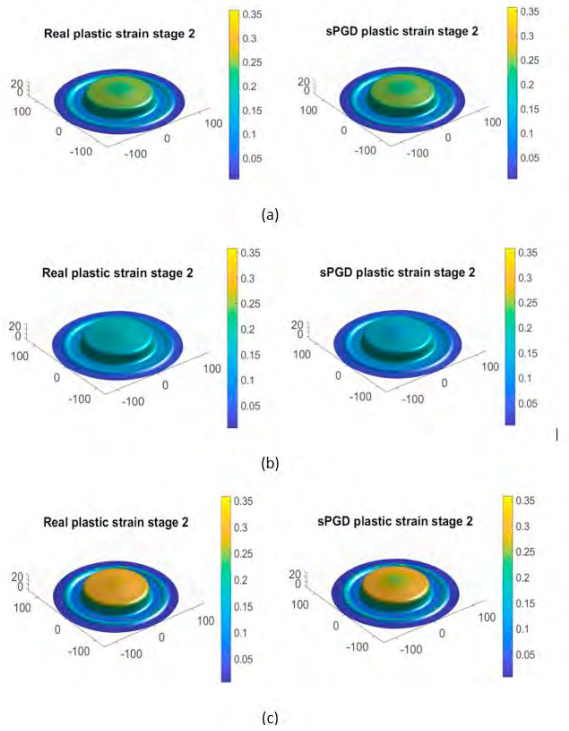

Fig. 6. Real (left) and predicted (right) displacement and plastic strain at the end of the second stage for three different input states $X^I(x)$ (same as Figs. 4 and 5), and combinations of the parameters F^{II}, ξ^{II} and μ^{II}.

$$u^M(x,\mu,\eta) = u^{M-1}(x,\mu,\eta) + X_M(x)\Psi_M(\mu)\,\Phi_M(\eta) \qquad (16)$$

with

$$u^{M-1}(x,\mu,\eta) = \sum_{k=1}^{M-1} X_k(x)\Psi_k(\mu)\Phi_k(\eta). \qquad (17)$$

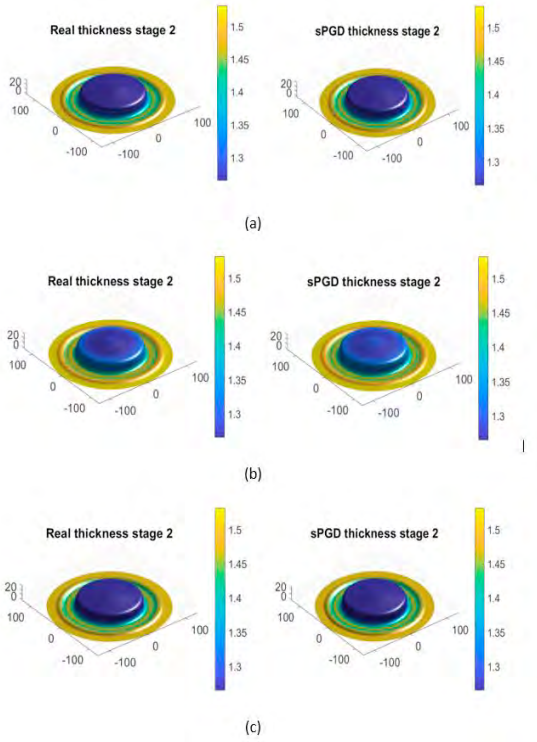

Fig. 7. Real (left) and predicted (right) displacement and thickness at the end of the second stage for three different input states $X^I(x)$ (same as Figs. 4 and 5), and combinations of the parameters F^{II}, ξ^{II} and μ^{II} (same as Fig. 6).

It is worth noting that the product of the test function $w(x,\mu,\eta)$ times the objective function $f(x,\mu,\eta)$ is only evaluated at few locations (the ones corresponding to the available data associated to the sampling). Since information is just known at P sampling points (μ_j,η_j), $j = 1,\dots,P$, it seems reasonable to express the test function not in a finite element context, but to express it as a set of Dirac delta functions collocated at the sampling points,

$$w(x,\mu,\eta) = (X_M(x)\Psi_M(\mu)\Phi_M(\eta))^* \sum_{j=1}^{P} \delta(\mu_j,\eta_j), \qquad (18)$$

where

$$(X_M(x)\Psi_M(\mu)\Phi_M(\eta))^* = X^*(x)\Psi_M(\mu)\Phi_M(\eta) + X_M(x)\Psi^*(\mu)\Phi_M(\eta) + X_M(x)\Psi_M(\mu)\Phi^*(\eta), \qquad (19)$$

giving rise to

$$\int_\Omega w(x,\mu,\eta)\big(u(x,\mu,\eta) - f(x,\mu,\eta)\big)dxd\mu d\eta = \int_\Omega (X_M(x)\Psi_M(\mu)\Phi_M(\eta))^* \sum_{j=1}^{P} \delta(\mu_j,\eta_j)\big(u(x,\mu,\eta) - f(x,\mu,\eta)\big)dxd\mu d\eta = 0. \qquad (20)$$

In the expression above nothing has been specified about the basis in which each one of the one-dimensional modes was

expressed. Two appealing choices, which tend to smooth the solution outside the control points, consists of using Chebyshev polynomials or interpolants based on Kriging techniques. In this work Chebyshev polynomials have been used but Kriging could be applied in order to avoid spurious oscillations characteristic of high order polynomial interpolation. This phenomenon is called Runge's phenomenon. It appears due to the fact that the sampling point locations are not chosen properly, i.e., they will not be collocated, in general, at the Gauss-Lobato-Chebyshev quadrature points. Kriging interpolants consider each point as a realization of a Gaussian process, so that high oscillations are considered as unlikely events.

The use of the sPGD in tandem with Chebyshev polynomials or Kriging interpolation of the one-dimensional functions allows excellent accuracy while drastically reducing the number of sampling points.

There are plenty of strategies to smartly select the position of the sampling points, but Latin Hypercube Sampling (LHS) [16] is chosen in the present work. Particularly, LHS tries to collocate P sampling points in such a way that the projection of those points into each axis are as far as possible while improving the coverage of the parametric space.

References

[1] Hey T, Tansley S, Tolle K. The Fourth Paradigm: Data-Intensive Scientific Discovery. Microsoft Research; 2009.

[2] Bur N, Joyot P, Ghnatios C, Villon P, Cueto E, Chinesta F. On the use of model order reduction for simulating automated fibre placement processes. Advanced Modeling and Simulation in Engineering Sciences; 2016;3.

[3] Chinesta F, Ladeveze P, Cueto E. A Short Review on Model Order Reduction Based on Proper Generalized Decomposition. Archives of Computational Methods in Engineering; 2011;18; p. 395-404.

[4] Chinesta F, Leygue A, Bordeu F, Aguado JV, Cueto E, Gonzalez D, et al. PGD-Based Computational Vademecum for Efficient Design, Optimization and Control. Archives of Computational Methods in Engineering; 2013; 20; p. 31-59.

[5] Chinesta F, Keunings R, Leygue A. The proper generalized decomposition for advanced numerical simulations. A primer. Springer; 2014.

[6] Chinesta F, Leygue A, Bognet B, Ghnatios C, Poulhaon F, Bordeu F, et al. First steps towards an advanced simulation of composites manufacturing by automated tape placement. International Journal of Material Forming; 2014;7.

[7] Chinesta F, Ladeveze P. Separated Representations and PGD-Based Model Reduction: Fundamentals and Applications. Springer; 2014.

[8] Chinesta F, Huerta A, Rozza G, Wilcox K. Model Order Reduction. Chapter in the Encyclopedia of Computational Mechanics, Second Edition, Erwin Stein, René de Borst & Tom Hughes Edt. John Wiley & Sons Ltd.; 2015.

[9] Ibañez Pinillo R, Abisset-Chavanne E, Chinesta F, Duval JL. A Multidimensional Data-Driven Sparse Identification Technique: The Sparse Proper Generalized Decomposition. Complexity; 2018; 2018:12; p. 1-11.

[10] Gonzalez D, Badias A, Alfaro I, Chinesta F, Cueto E. Model order reduction for real-time data assimilation through Extended Kalman Filters Comput. Methods Appl. Mech. Eng.; 2017; 326; p. 679–693.

[11] Chinesta F, Cueto E, Abisset-Chavanne E, Duval JL, Khaldi FE. Virtual, Digital and Hybrid Twins: A New Paradigm in Data-Based Engineering and Engineered Data. Archives of Computational Methods in Engineering; 2018.

[12] Quaranta G, Abisset-Chavanne E, Chinesta F, Duval JL. A cyber physical system approach for composite part: From smart manufacturing to predictive maintenance. ESAFORM2018 Conference, AIP Conference Proceedings; 2018; 1960:1.

[13] Brunton S, Proctor J, Kut N. Discovering governing equations from data by sparse identification of nonlinear dynamical systems. Proc Natl Acad Sci USA; 2016; 113; p. 3932-3937.

[14] Kutz JN. Data-driven modeling & scientific computation: Methods for complex systems & big data. Oxford University Press, Inc., New York, NY, USA, 2013.

[15] Ibañez R, Abisset-Chavanne E, Aguago JV, Gonzalez D, Cueto E, Chinesta F. A manifold learning approach to data-driven computational elasticity and inelasticity. Arch. Comput. Methods Eng; 2018; 25; p. 47–57.

[16] McKay M, Beckman R, Conover W. A comparison of three methods for selectingvalues of input variables in the analysis of output from a computer code. Technometrics; 1979; 21; p. 239–245.